Systems Engineering for the Preliminary Design of the Thirty Meter Telescope

George Z. Angeli*[a], Scott Roberts[b], and Konstantinos Vogiatzis[a]
[a] Thirty Meter Telescope Observatory, 1200 E. California Blvd. Mail Code 102-8, Pasadena, CA, USA 91125;
[b] Herzberg Institute of Astrophysics, 5071 West Saanich Road, Victoria, BC Canada V9E 2E7

ABSTRACT

A large ground-based astronomical telescope project, like the Thirty Meter Telescope (TMT), is rivaling space projects in technical complexity, design and construction time span, budget, as well as organizational diversity and geographical distribution. A unique challenge in large ground based projects is implementing appropriate systems engineering methods and tools in the absence of the strong institutional backdrop that space projects can rely on. This paper provides a critical overview of the established system engineering practice in the TMT project, including requirements engineering, document and configuration control, as well as performance allocation and estimation. In particular, we introduce a new performance metric, the Point Source Sensitivity (PSS), and show how it is superior to the 80% enclosed energy diameter measure. The overall strategy for estimating the performance of TMT is outlined, showing how the various elements of performance modeling, reported in detail in other papers, fit together to provide a probabilistic assessment of the achievable image quality of the observatory. An overview of the estimated system performance is presented with critical analysis of the major factors limiting the seeing limited and AO aided observations.

Keywords: Thirty Meter Telescope, requirements engineering, performance allocation, performance estimate, end-to-end modeling

1. INTRODUCTION

The design philosophy of the Thirty Meter Telescope Observatory [1] is based on the conviction that the development and implementation of a 30 meter, near diffraction limited telescope is above all a system challenge. It requires the seamless integration of the telescope, the adaptive optics systems and the instruments, which in turn precipitates the need for an integrated design approach. Our approach takes into account simultaneously a whole range of issues: various site characteristics, enclosure configuration, telescope structural layout; orchestrating a complex control system driving active and adaptive optical elements; fabricating, polishing, controlling, and maintaining the primary, secondary, and tertiary mirror surfaces; and distributing these functionalities among the various subsystems.

The single most important technological achievement of the last decades has been the explosion of computing power and matching evolution of computing algorithms. The most visible example of reducing physical robustness by improved computations was the emergence of altitude-azimuth mounts, enabled by the fast and precise conversion of sky coordinates into telescope horizontal coordinates. Active optics, the real time adjustment of optical surface shapes and adaptive optics, the real time correction for the optical effects of atmospheric turbulence are well known examples of this trend.

Systems engineering benefits from the widespread use of powerful computers through the technical feasibility of all-electronic documents and drawings databases as well as the emergence of new software tools capable of organizing, linking, and visualizing the complex relationships among requirements, design elements, and test procedures.

However, the really transformational change in systems engineering is in system modeling, where the emergence of new computing capabilities opened new windows to more thorough optimization and early verification of the design. The TMT project takes full advantage of this new trend. As described later in the paper, we developed a complex and powerful simulation framework capable of evaluating together the various aspects of the system.

*gangeli@tmt.org

2. REQUIREMENT ENGINEERING AND CONFIGURATION MANAGEMENT

The TMT observatory requirements are represented at the highest level by the TMT Science Requirements Document (SRD). This document is translated into three system engineering level documents, the Operations Concept Document (OCD) [2], the Observatory Requirements Document (ORD) [3] and the Observatory Architecture Document (OAD) [4]. The requirements documented in the OCD and the ORD fully describe the top level engineering requirements and operational concepts to satisfy the criteria of the Science Requirements Document, and by reference, the Science Case for the Observatory. The OCD is used as guidance for the design and implementation of TMT operations processes and staffing plan, while the ORD provides the top level engineering function and performance requirements of the observatory. The OAD defines the top level architecture for the observatory, and the decomposition of the observatory into subsystems. It documents the system wide implementation decisions and details, and system budgets, and partitions function and performance requirements among the subsystems, and describes the highest level interfaces as necessary to ensure the integrated systems level performance of the observatory.

Below the System Level, the observatory has been decomposed into 35 subsystems, each an individually deliverable and testable system, with its own design requirements document, and documented interfaces with other systems. The subsystem design documents will address the requirements and interfaces at the subsystem and system level. Test plans will be developed for each subsystem and for the observatory system as a whole. The project documentation is illustrated in Figure 1. The project also maintains an N^2 diagram document to specify track the interfaces between the subsystems.

.

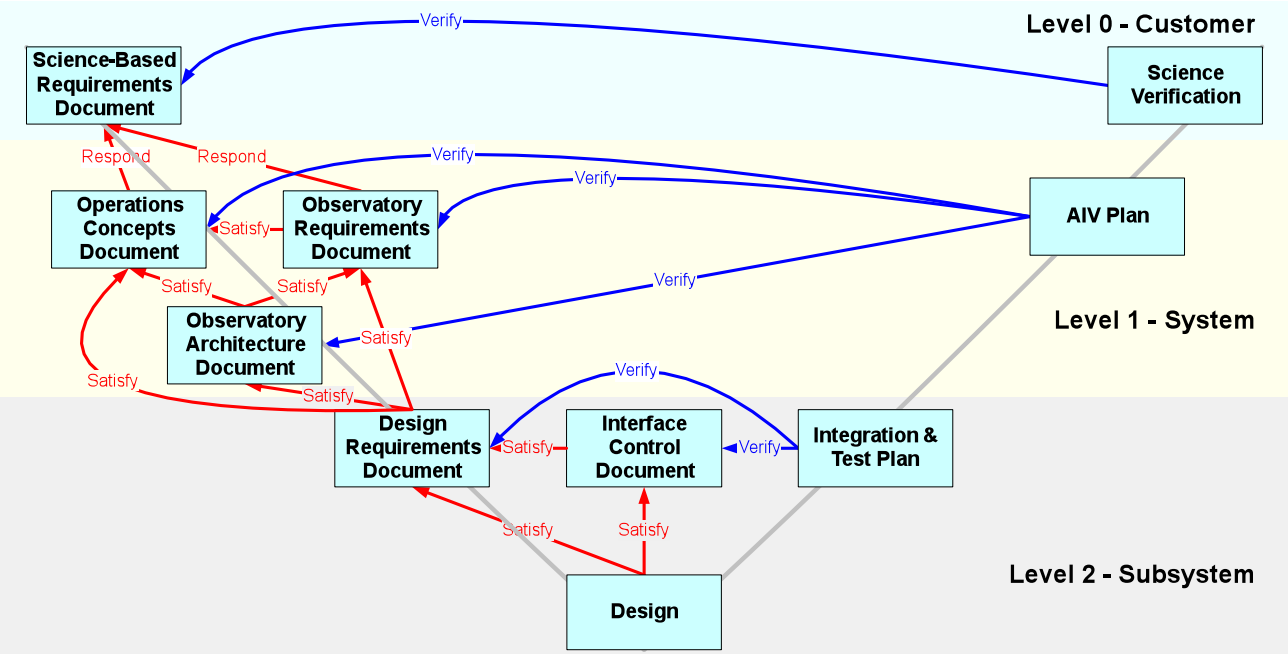

Figure 1 - Systems engineering lifecycle V-diagram for TMT

The TMT project is following a standard process for formal requirements definition and flow down. Each requirement is individually numbered, and the flow down of the requirements through DRDs, ICDs, and verification plans is documented. To aid with the requirements engineering process, a DOORS database is being implemented to record the requirements, plus their flow-down, traceability, and verification method. The official requirements for the project are represented as change controlled stand-alone documents, with the DOORS database paralleling the released requirements documents. The overhead of maintaining duplicate copies of requirements is eased by DOORS ability to ingest and output requirements to several document formats, and by its tools for revision control and baselining. The

DOORS database will be a tool used by systems engineering, and reports will be generated for the project. An html version of the TMT DOORS requirements database, with hyperlinks to enable tracing of requirements up and down will be available to all TMT staff and partners. A schema for the DOORS database implementation is shown in Figure ???.

The current documentation status is that the system level documents are all released and under change control. The project has a subset of the subsystem DRDs under change control, and is working towards placing the majority of the subsystem DRDs and ICDs under change control by the project PDR, planned for early in 2009. For project PDR we also plan to have the observatory test and verification plan developed.

The project has developed procedures to establish and maintain the consistency of our system documentation and engineering data. The TMT Documentation Plan describes the project documentation that will be formally controlled, and establishes the process for the change control of documents such as DRDs and ICDs. The change control process is designed to be efficient so that lower level documents can be updated with a minimum of overhead. As changes become more significant from either a design, cost or schedule perspective, the rigor of the change control process increases. For major decisions there is a formal change control board process established. The documentation plan also defines the document numbering standard and the document management using the DocuShare system. Currently, the system level requirements documents undergo revision on approximately a monthly basis, with the bulk of the changes occurring in the OAD as the design evolves.

The project has also established standards and procedures for CAD Models. This includes templates and standards for the preparation of CAD models, a master geometry model that is used for assembling the overall observatory CAD model from the constituent subsystem models. A process is established that allows partners and vendors to work in their own STEP compliant CAD systems, and to interface with the project's SolidWorks CAD database. CAD assemblies, parts and drawings are stored in a Product Data Management system, which is also used to store other engineering data such as finite element models.

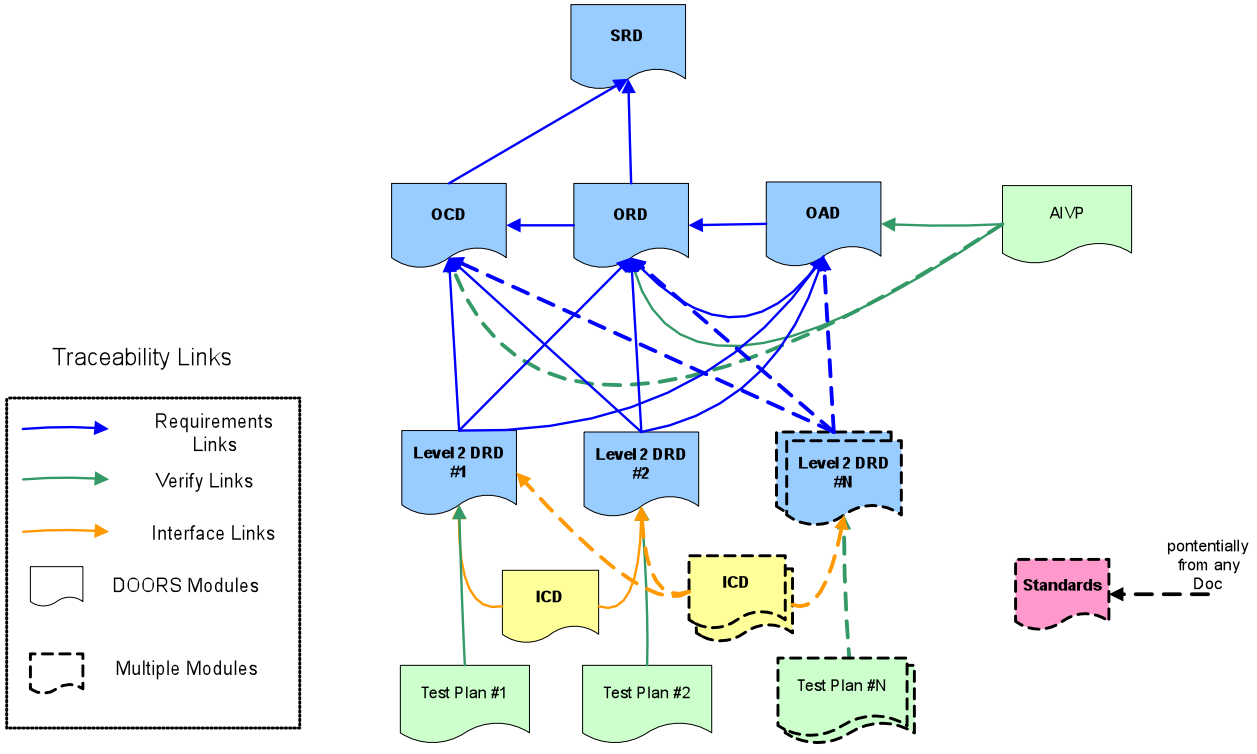

Figure 2 – DOORS Requirements Database Schema

3. SEEING LIMITED IMAGE QUALITY METRIC

In order to evaluate image quality, it needs to be measured. For seeing limited observations, when the wavefront error is relatively large and its spatial bandwidth is wide, first order statistical properties, like standard deviation (RMS) of the wavefront are not adequately characterizing the optical effect of the aberration. Indeed, it is more meaningful to derive metrics directly from the focal plane behavior of the system. Practically all the image quality metrics recently used for characterizing seeing limited image quality are attempts to capture the essence of the Point Spread Function (PSF) in a single number measure.

Besides the wavefront error and PSF, another way to characterize an optical system is through its Optical Transfer Function (OTF) establishing a relationship between the spatial Fourier spectra of aberrated and geometric image intensities (I_{ag} and).

$$|OTF| \qquad (2.1)$$

A linear system model based on the OTF is shown in Figure 3. As system performance of an advanced telescope depends on various feedback loops, the figure is constructed to reflect modern control architecture. Since the OTF and PSF are Fourier transform pairs, any image quality metric derived for the PSF can also be expressed in terms of the OTF.

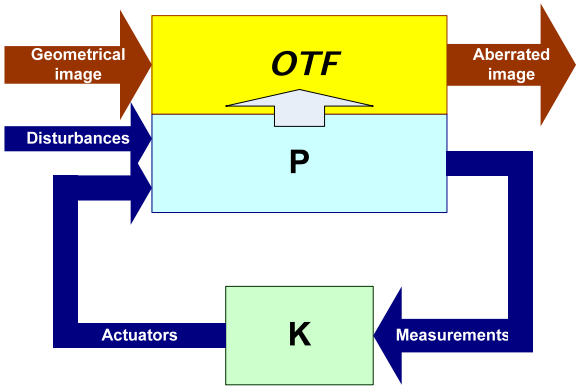

Figure 3 - Linear model of the optical system. "***P***" represents the "plant", i.e. the observatory and atmosphere, while "***K***" denotes the feedback loops: guiding, active and adaptive optics

3.1 Metrics based on the central value of the PSF

As the image quality of an optical system degrades, its PSF spreads wider. By definition the integral of the PSF is unity, so the central value of an aberrated system, i.e. the PSF value on the optical axis is lower than that of a perfect system. This realization led to a simple but quite powerful image quality metric, the Strehl ratio, *S*. As expected, for small wavefront aberrations with relatively uniform spatial frequency distribution, the Strehl ratio is directly related to the variance of the wavefront, O^2 through the Maréchal approximation. It is also straightforward to show that the Strehl ratio can be calculated from the OTF of the system.

$$S \approx \frac{PSF_{total}(0)}{PSF_{perf}(0)} \approx \frac{\int |OTF_{total}|\, dH}{\int |OTF_{perf}|\, dH} \approx e^{-2O^2} \qquad (3.1)$$

However, for systems dominated by large atmospheric aberrations, like ground based telescopes, the Strehl ratio is inconveniently small. Brown [5] and later independently Dierickx [6] suggested further normalizing the system Strehl ratio with that of the perfect telescope S_0 including the atmosphere. Javier-Castro [7] pointed out that the metric defined in such a way, called Central Intensity Ratio (CIR) retains the multiplicative property of the Strehl ratio, i.e. the overall CIR can be approximated by multiplying the CIRs corresponding to different optical errors. For a given wavelength and atmospheric seeing *N* (FWHM of the PSF), the CIR depends primarily on the variance of the wavefront slope, O_s^2.

$$CIR = \frac{S}{S_0} \approx \frac{PSF_{total}(0)}{PSF_{atm}(0)} \approx \frac{\int |OTF_{total}|\, dH}{\int |OTF_{atm}|\, dH} \approx 12.9\, O_s^2 N^2 \qquad (3.2)$$

While both the Strehl ratio and CIR are widely and successfully used (the VLT error budget was expressed in CIR), neither of them accounts for the shape of the PSF outside of its core. As long as the optical aberrations to be compared by using these metrics have similar spatial frequency content, this limitation is negligible. However, for ground based

telescopes this requirement is hardly met. Mirror support print through, for example has much more high spatial frequency content than mirror thermal deformation, not to mention telescope mirror misalignments.

3.2 Metrics based on the area of the PSF

Instead of relying on a single, although very characteristic point of the PSF, a family of performance metrics evokes an equivalent area of the PSF, i.e. the spot size of the image of a point source. As indicated below, there are various ways to define an equivalent area:

- FWHM (Full Width at Half Maximum) simply "cuts" the PSF cone in half in height and measures the equivalent diameter of the cut surface. While this measure practically defines an area, similarly to the central value metrics it does not consider the shape of the wings of the PSF.
- D_{80}, the diameter encircling 80% of the light energy partially remedies this problem, as it relies on the integral of the entire PSF in defining an equivalent spot size. This metric is widely used: both Keck and Gemini were design by error budgets expressed in D_{80}. The original TMT error budget was also formalized in D_{80}.

  Unfortunately, for PSFs of small aberrations still showing the residual of the Airy rings, D_{80} as the function of wavefront error behaves irregularly. When used for error budgeting, the individual component D_{80} displays a dip by crossing the dark ring with increasing strength of the aberration. This dip is obviously not physical, as the given small error never occurs by itself, i.e. the Airy ring does not exist.
- The Equivalent Noise Area (*ENA*) as image quality metric was suggested by King [8]. *ENA* links the equivalent area definition to an astronomical measure, the intensity variance σ_{int}^2 of a background limited point source observation. King shows that for a given source intensity I and background irradiance b the intensity variance, i.e. the photometric error depends on the shape of the PSF.

$$\sigma_{\text{int}}^2 = \frac{I}{\int\int \frac{PSF^2}{PSF + b/I}\, d\in} \tag{3.3}$$

  At the limit of background limited observation, where $bI \gg$, Equation (3.3) gives the definition of ENA.

$$\sigma_{\text{int}}^2 = \frac{b}{\int\int PSF^2 \, d} \quad ENA = bENA, \text{where} \quad \frac{1}{} \tag{3.4}$$

  Occasionally the inverse of *ENA* is called "sharpness" [9].

Besides its capability of characterizing the PSF, a metric's worth depends also on how well it can be used for error budgeting, i.e. combining the optical effects of various imperfections. It is widely assumed that PSF equivalent areas like D_{80}^2 and ENA are additive, meaning the equivalent areas of various statistically independent aberrations can be added up to estimate their joint effect. While this is a reasonably good approximation if the different errors are small and comparable in strength, this linear approximation breaks down for cases where one effect is clearly dominant. For ground based telescopes atmospheric aberration is overwhelmingly larger than any other optical error, resulting in nonlinear behavior: the equivalent PSF area corresponding to a given aberration depends not only on the given aberration but also on the underlying atmospheric wavefront error.

Figure 4 shows *ENA* values corresponding to lateral segment support print through of 12nm$_{\text{RMS}}$, calculated with the assumption of additively combining print through with different underlying atmospheric aberrations: $ENA = ENA_{\text{combinedatmosphere}}$. It is noteworthy that *ENA*, i.e. the optical contribution of print through is getting better (smaller) as the atmosphere improves (r_0 is getting larger), which is actually counterintuitive.

The calculation errors due to neglecting this nonlinearity can be significant (>10%). A sensible way of handling this nonlinearity can be normalizing the metric to the perfect telescope including atmospheric turbulence, similarly to the normalization of CIR. Besides making the nonlinear feature clearly appreciable, this normalization leads to a more intuitive atmospheric dependence: a given telescope error results in a more pronounced optical effect if the atmosphere is better.

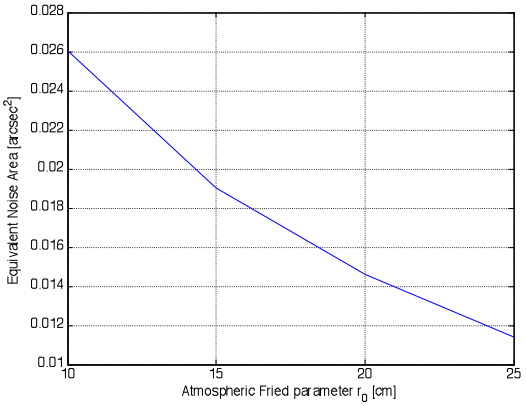

Figure 4 – Equivalent Noise Area as the function of atmospheric r_0.

3.3 The Point Source Sensitivity metric

Considering the advantages and shortcomings of the various metrics, TMT developed a new metric having its roots as much in linear system theory as in optical analysis.

Considering the linear system in Figure 3, the objective of system design as well as the ***K*** feedback control is to optimize the ***P-K*** system in the sense of "maximizing" the normalized intensity spectrum of the output (aberrated image) for all inputs, that is "maximizing" the "size" of the system. In this statement "size" and "maximum" are notional, as they are not yet defined.

In linear system theory, "size" is associated with norms. There are various ways to define norms in a linear space, but probably the most usual and useful is based on the generalized concept of power, or RMS (no mean removed) value. For systems it is called the H_2 norm denoted as $\| \ \|_2$ and defined by the square integral of the transfer function, in our case the OTF.

$$\|OTF\|_2 = \sqrt{\int\int |OTF|^2 \, df_x df_y} = \sqrt{\int\int MTF^2 \, df_x df_y} \tag{3.5}$$

Here the Modulation Transfer Function (MTF) is the modulus of the OTF: $MTF = |OTF|$.

Indeed, assuming a point source at infinity with normalized intensity spectrum of 1, the H_2 norm of the OTF is the spatial RMS intensity at the focal plane.

$$\|OTF\|_2 = \sqrt{\int\int |OTF \cdot 1|^2 \, df_x df_y} = \sqrt{|\text{image}|^2} \tag{3.6}$$

The same physical interpretation can also be reached by invoking Parseval's Theorem. Since the OTF and PSF are Fourier transform pairs, their absolute square integrals are equal. Consequently, the square of the H_2 norm is the inverse of the ENA.

$$\|OTF\|_2^2 = \int\int MTF^2 \, df_x df_y = \int\int PSF^2 \, dx dy \qquad \frac{1}{ENA} \tag{3.7}$$

As discussed earlier, normalization to the perfect case including only atmospheric aberrations and inherent telescope diffraction is beneficial to keep the actual metric values close to the unity and ensure intuitive behavior. The normalized metric TMT is using called Point Source Sensitivity (PSS).

$$PSS = \frac{\left\|\mathbf{OTF}_{\text{total}}\right\|_2^2}{\left\|\mathbf{OTF}_{\text{atm}}\right\|_2^2} \quad \frac{\int PSF_{\text{total}}^2 \, d\in}{\int PSF_{\text{atm}}^2 \, d\in} \tag{3.8}$$

The behavior of the PSS metric is detailed elsewhere [10]. One of its most important features is its multiplicative character. With good approximation, for a given atmosphere the product of the PSS values corresponding to the different telescope errors provides the overall PSS value of the system.

It is worth to mention that for small, spatially uncorrelated wavefront errors, like the output of an AO system, the PSS metric approaches the square of the Strehl Ratio.

3.4 The Science Productivity Metric

While the PSS provides a good metric for photometric performance degradation due to local effects, like telescope errors or thermal seeing, it does not differentiate between the actual values of the photometric error. However, the *ENA* can be used to formalize another quantitative metric placing a premium on good overall image quality. A Science Productivity Metric (SPM) can be defined as the ratio of the average H_2^2 of the entire aberrated system, including the atmosphere, to that of the perfect system, including atmosphere and telescope inherent diffraction errors only.

$$SPM = \frac{\left\langle \left\|\mathbf{OTF}_{\text{total}}\right\|_2^2 \right\rangle}{\left\langle \left\|\mathbf{OTF}_{\text{atm}}\right\|_2^2 \right\rangle} \tag{3.9}$$

Here <> denotes ensemble, i.e. long term time average over all environmental and operating conditions.

Unfortunately, the SPM is not suitable for error budgeting, as multiplicatively combining various error effects at the ensemble average level is not correct. We know that the PSS metric is multiplicative for time periods maintaining the assumption of statistically independent errors.

$$PSS_{\text{total}} = \frac{\left\|\mathbf{OTF}_{\text{total}}\right\|_2^2}{\left\|\mathbf{OTF}_{\text{atm}}\right\|_2^2} \prod_{i=1}^{N} \frac{\left\|\mathbf{OTF}_{i+\text{atm}}\right\|_2^2}{\left\|\mathbf{OTF}_{\text{atm}}\right\|_2^2} \tag{3.10}$$

Equation (3.10) indicates that H_2 norm squares are not multiplicative: $\left\|\mathbf{OTF}_{\text{total}}\right\|_2^2 \neq \prod_{i=1}^{N} \left\|\mathbf{OTF}_{i+\text{atm}}\right\|_2^2$. It is straightforward to show now that SPM is indeed not multiplicative for different errors, as $PSS_i = \frac{\left\|\mathbf{OTF}_{i+\text{atm}}\right\|_2^2}{\left\|\mathbf{OTF}_{\text{atm}}\right\|_2^2}$ and $\left\|\mathbf{OTF}_{\text{atm}}\right\|_2^2$ are certainly not statistically independent.

$$SPM = \frac{\left\langle \left\|\mathbf{OTF}_{\text{total}}\right\|_2^2 \right\rangle}{\left\langle \left\|\mathbf{OTF}_{\text{atm}}\right\|_2^2 \right\rangle} \neq \frac{\left\langle \left\|\mathbf{OTF}_{\text{atm}}\right\|_2^2 \prod_{i=1}^{N} \frac{\left\|\mathbf{OTF}_{i+\text{atm}}\right\|_2^2}{\left\|\mathbf{OTF}_{\text{atm}}\right\|_2^2} \right\rangle}{\left\langle \left\|\mathbf{OTF}_{\text{atm}}\right\|_2^2 \right\rangle} = \prod_{i=1}^{N} \frac{\left\langle \left\|\mathbf{OTF}_{i+\text{atm}}\right\|_2^2 \right\rangle}{\left\langle \left\|\mathbf{OTF}_{\text{atm}}\right\|_2^2 \right\rangle} \tag{3.11}$$

However, it is certainly feasible to calculate SPM, making it practical to use this metric in system trade studies and performance evaluation, concurrently with the PSS metric. They illuminate different aspects of the design: while PSS shows the balance between the various error sources, SPM links the overall performance to the science capability of the observatory.

It is worth to note that for TMT, in good approximation [11] the average PSS of the system is the product of the average PSSs corresponding to the various error terms, indicating relatively low statistical correlation among these error terms.

$$\langle PSSPSS_{total} \rangle \cong \int_{i=1}^{N} \langle \quad \rangle \tag{3.12}$$

4. MODELING ARCHITECTURE FOR SEEING LIMITED IMAGE QUALITY ASSESSMENT

The objective of system performance modeling is to evaluate the optical effects of various implementation imperfections and disturbances. By considering the specified level of the imperfections and the expected level of disturbances as requirements, the modeling process can be perceived as the validation of these requirements. Modeling can provide the proof for the entire system meeting its requirements if all the subsystems are meeting theirs.

The imperfections and disturbances can be categorized according to their statistical properties. There are some *deterministic,* even *constant* effects:

- Optical design residual errors, in particular off-axis astigmatism inherent with the Ritchey-Chrétien design
- Diffraction effects due to the finite aperture, segmentation, and pupil obscuration

Some other *deterministic errors* are *randomized* by environmental and operational parameters:

- Mirror support print through randomized through telescope zenith angle
- In-plane segment motion randomized through telescope zenith angle, and ambient temperature
- Thermal deformations of optical surfaces and support structures randomized through ambient and local temperature

Most of the imperfections and disturbances are *true random processes*, although their statistical properties may depend on environmental and operational parameters:

- Wind buffeting with telescope zenith and azimuth angle, as well as external wind speed dependency
- Dome and mirror seeing with zenith and azimuth angle, as well as temperature and external wind speed dependency
- Local actuator and sensor noise and drift
- APS measurement errors
- Material and fabrication errors (polishing error, CTE variation, installations errors, etc.)

Due to the random nature of the disturbances and imperfections, as well as to the statistical correlations through wind, telescope orientation, and thermal effects, the performance of the observatory can be addressed in a stochastic framework only. The performance, expressed in PSS is a random variable that can be characterized by its stochastic parameters.

Furthermore, the thermal processes influencing several of the disturbances and imperfections imply system memory due to the several hour long thermal time constants of the mirrors and structural elements [12]. Consequently, the statistical approach used should operate in the time domain.

The time domain Monte Carlo simulation we developed utilizes a long time record, we call it “standard year”, in order to capture a representative ensemble of environmental and operational parameters. The time histories of environmental parameters were captured by our site testing equipment at the reference site, Armazones. The relevant parameters are:

- External wind speed and direction, as well as its height profile
- External air temperature and its height profile
- Atmospheric Fried parameter (r_0) in zenith direction

Operational parameters, as telescope elevation and azimuth angles were extracted from a year of Gemini North record. While the entire night time history was considered for thermal modeling, only observing time was included in the performance estimate.

The three major blocks of the framework are the (i) aero-thermal, (ii) quasi-static optical, and (iii) dynamic modules. Each of these modules has its own PSS post-processor providing the metric to be combined with the rest of the errors. Each of these modules are described in details elsewhere: [13], [14], [15], [16], and [17].

Although it is perceivable to run the entire model for each time interval in the standard year, it would result in an enormous computer simulation run, which is certainly not practical. The problem is not just the required computing

power and the potential fragility of such a big integrated code, but above all the long calculation time preventing the flexible use of the simulations to support trade studies.

We decided to pre-calculate characteristic results of the modules and place these into a LUT, as seen in **Figure 5**. At the Monte Carlo run, the actual values used are interpolated from the LUT values. Obviously, the basic thermal model addressing the thermal memory of the system cannot be pre-calculated; it is simulated in the Monte Carlo kernel.

The time step for the base kernel is 2 minutes. Although it is long enough to support the "long exposure OTF" approximation used in some of the PSS calculations, but short enough to consider the input parameters quasi-constant and consequently independent, its actual value was determined by the sampling rate of the environmental and operational parameters.

The details of this framework are described elsewhere [11].

The adaptive optics simulations were linked to the telescope models through a manual pipeline. The mean shapes and positions of the various mirrors were implemented in the AO beam path and corrections were estimated. For dynamic image jitter, the temporal PSD was approximated by the telescope dynamic integrated model and further compensated by the AO fast tip/tilt stage. Since the AO off-load or OIWFS global loop was implemented only by its required performance (residual error), the pipeline architecture does not restrict the validity of the simulations.

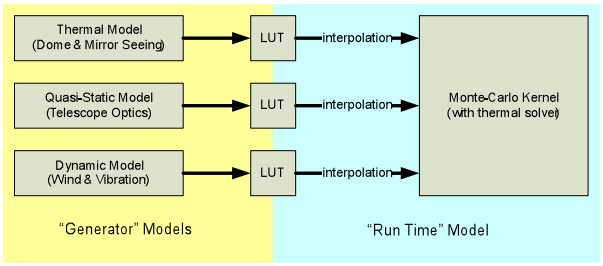

Figure 5 - Actual architecture of the Monte Carlo simulation framework

5. MAJOR SIMULATION RESULTS

The Science Productivity Metric for the current design, calculated from the modeled aberrations is 0.8178. As shown in Figure 6, the modeled components of observatory performance as expressed in mean PSS over all environmental and operational conditions is 0.8571. By combining it with the error budget allocations for the not modeled effects, the overall TMT performance is expected to be 0.8415. The cumulative probability distributions and mean values of various error components are reported elsewhere [11].

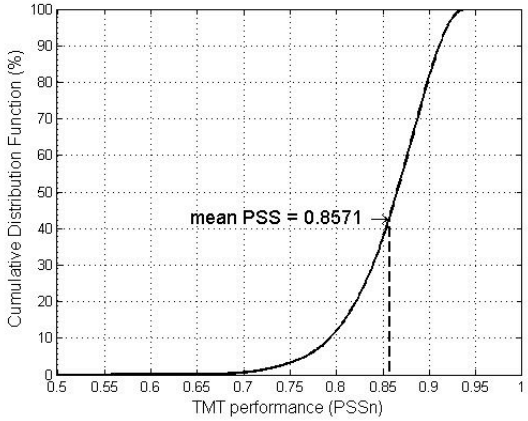

Figure 6 - Cumulative Probability Distribution (CDF) of PSS over all environmental and operational parameters considered

Another way to quickly assess the distribution of system performance among different error sources is to choose a representative configuration and estimate the performance corresponding to that configuration. Zenith angle of 30° and a temperature difference of 2°C between system alignment and observation are close to the median values as derived from the standard year. Using these values as input for estimating the individual error budget categories, the rolled up system performance (0.8440) is very close to the stochastic mean (0.8415); actually, the difference is ~0.3% only.

Using the snapshot error distribution corresponding to the representative parameters set, the major error contributors can be identified, as shown in Figure 7. As expected, the major contributor is primary mirror (segment) figuring residual. The second tier of errors includes thermal seeing, primary mirror print through, M2 and M3 shapes, and M1 segment alignment errors.

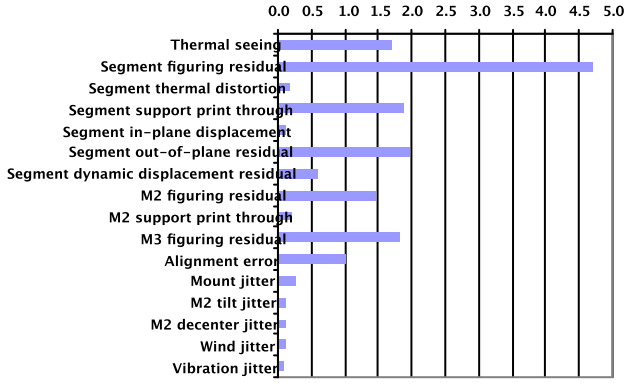

Figure 7 - Major error contributors expressed in 100(1-PSS) for r_0 of 20cm, zenith angle of 30° and temperature difference between APS measurement and observation of 2°C

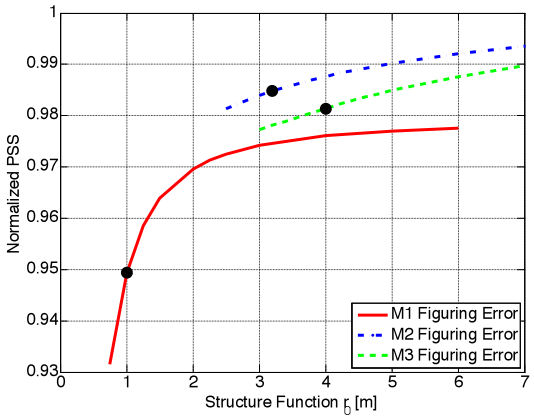

Figure 8 – Performance sensitivities to mirror shape specifications expressed as atmosphere like structure function characterized by the associated r_0 value. The black dots mark the current mirror specifications.

Looking for potential performance improvement, mirror shapes seem to be reasonable candidates. For TMT, mirror polishing errors are currently specified by tilt removed structure functions. For the three mirrors, Figure 8 shows the sensitivities of their respective PSS values to r_0 of the specified wavefront structure functions. It is clear that segment shape error is not just the tallest pole in the budget but it is also the most sensitive to surface specifications.

6. CONCLUSIONS

The TMT project developed modeling tools to estimate the bottom-up performance of the observatory and evaluate trade studies. These tools include (i) a high spatial resolution optical model of the telescope and telescope errors, (ii) dome and mirror seeing models based on aero-thermal and solid thermal simulations, and (iii) a dynamic integrated model comprising a complex wind model. These individual models are tied together in a stochastic framework.

The project settled with a new, advanced performance metric, the Point Source Sensitivity, which (i) properly accounts for the spatial frequency distribution of the wavefront errors, (ii) is conceptually tied to the photometric error of point source observations, and (iii) fully multiplicative to support error budgeting. Another, closely related metric was established to quantitatively evaluate the science requirement for seeing limited observations.

The project needs to look into tightening the requirements in order to improve the Science Productivity Metric. The simulations reported at this review indicate that the effects should be further investigated are:

i. Dome and mirror seeing;
ii. Mirror figuring residuals, in particular segment figuring residuals after active optics correction;
iii. Alignment and phasing errors dominating the "Segment out-of-space residual" and "Alignment error" categories.

A few years ago one of the major concerns regarding the feasibility of extremely large telescopes was wind buffeting. Both of our own simulations and those of other groups showed significant image degradation, mostly image motion due to wind. From the very beginning of the design process, our project assigned top priority to resolving wind buffeting. Consequently, the resulting design mitigates wind effects to acceptable level.

While we are aware of the importance of equipment induced and micro-seismic vibrations, our current estimates carry significant uncertainties due to the uncertainties of the input parameters. We are in the process of collecting further data at Keck Observatory that will be used to improve these estimates.

7. ACKNOWLEDGEMENTS

The authors are grateful to Jerry Nelson, TMT Observatory Scientist for his original suggestion to consider the Equivalent Noise Area and for all the useful and exciting discussions about performance metrics. The authors acknowledge the contributions of the TMT Systems Engineering team; Douglas MacMynowski, Mitchell Troy, Carl Nissly, Byoung-Joon Seo, and John Pazder provided useful comments and suggestions, as well as most of the simulation results summarized in this paper.

The TMT Project gratefully acknowledges the support of the TMT partner institutions. They are the Association of Canadian Universities for Research in Astronomy (ACURA), the California Institute of Technology and the University of California. This work was supported as well by the Gordon and Betty Moore Foundation, the Canada Foundation for Innovation, the Ontario Ministry of Research and Innovation, the National Research Council of Canada, the Natural Sciences and Engineering Research Council of Canada, the British Columbia Knowledge Development Fund, the Association of Universities for Research in Astronomy (AURA) and the U.S. National Science Foundation.

REFERENCES

[1] Thirty Meter Telescope Construction Proposal, http://www.tmt.org/news/TMT-Construction%20Proposal-Public.pdf
[2] Operations Concept Document, http://www.tmt.org/foundation-docs/TMT-OCD-CCR6.pdf
[3] Observatory Requirements Document, http://www.tmt.org/foundation-docs/ORD-CCR18.pdf
[4] Observatory Architecture Document, http://www.tmt.org/foundation-docs/OAD-CCR17.pdf
[5] Referenced by R.N. Wilson, "Reflecting Telescope Optics II", Springer **1999**
[6] P. Dierickx, "Optical Performance of Large Ground-based Telescopes", Journal of Modern Optics, pp569-588
[7] Javier Castro *et al*., "Image Quality and Active Optics for the Gran Telescopio Canarias", Proc. SPIE Vol. 3352, p. 386-399, Advanced Technology Optical/IR Telescopes VI, Larry M. Stepp; Ed.
[8] I. R. King, "Accuracy of Measurement of Star Images on a Pixel Array", Publications of the Astronomical Society of the Pacific, **95**, pp163-168, **1983**
[9] Pierre Y. Bely; Ed., "The Design and Construction of Large Optical Telescopes", Springer **2002**
[10] B. J. Seo *et al*. "Analysis of Point Source Sensitivity as a Performance Metric for the Thirty Meter Telescope", Proc. SPIE Vol. 7017 (to be published)
[11] K. Vogiatzis, G.Z. Angeli, "Monte Carlo Simulation Framework for TMT", Proc. SPIE Vol. 7017 (to be published)
[12] M. Cho, *et al*., "Thermal Performance Prediction of the TMT Optics ", Proc. SPIE Vol. 7017 (to be published)
[13] C. R. Nissly, *et al*. "High-Resolution Optical Modeling of the Thirty Meter Telescope for Systemic Performance Trades", Proc. SPIE Vol. 7017 (to be published)
[14] D. G. MacMynowski, C. Blaurock, G.Z. Angeli, "Dynamic Analysis of TMT", Proc. SPIE Vol. 7017 (to be published)
[15] K. Vogiatzis, "Advances in Aero-Thermal Modeling for TMT", Proc. SPIE Vol. 7017 (to be published)
[16] D. G. MacMynowski, P.M. Thompson, M. Sirota, "Analysis of TMT Primary Mirror control Structure Interaction", Proc. SPIE Vol. 7017 (to be published)
[17] J.S. Pazder, K. Vogiatzis, G.Z. Angeli, "Dome and Mirror Seeing Estimates for the Thirty Meter Telescope", Proc. SPIE Vol. 7017 (to be published)